

Energy stabilization of the *s*-symmetry superatom molecular orbital by endohedral doping of C₈₂ fullerene with a lanthanum atom

Min Feng,¹ Yongliang Shi,² Chungwei Lin,^{1,*} Jin Zhao,^{1,2} Fupin Liu,³ Shangfeng Yang,³ and Hrvoje Petek^{1,†}

¹*Department of Physics and Astronomy, University of Pittsburgh, Pittsburgh Pennsylvania 15260, USA*

²*Hefei National Laboratory for Physical Sciences at Microscale and Department of Physics, University of Science and Technology of China, Hefei, Anhui 230026, P. R. China*

³*Hefei National Laboratory for Physical Sciences at Microscale, CAS Key Laboratory of Materials for Energy Conversion and Department of Materials Science and Engineering, University of Science and Technology of China (USTC), Hefei, Anhui 230026, P. R. China*

(Received 5 June 2013; published 14 August 2013)

Energy stabilization of the superatom molecular orbitals (SAMOs) in fullerenes is investigated with the goal of involving their nearly free-electron bands in practical charge transport applications. Combining low-temperature scanning tunneling microscopy-based spectroscopic methods and density functional theory calculations on an endohedral metallofullerene La@C₈₂, we confirm that the *s*-SAMO of C₈₂ fullerene is stabilized by as much as 2 eV with respect to that of C₆₀ by endohedral doping with the La atom. On the copper metal substrate, the *s*-SAMO energy is further lowered to just 1 eV above the Fermi level, making the applications of *s*-SAMO state in transport more plausible. We conclude that in an endohedral metallofullerene, the *s*-SAMO state is stabilized through the hybridization with the *s*-symmetry valence state of the metal atom and the stabilization energy correlates with the ionization potential of the free atom.

DOI: [10.1103/PhysRevB.88.075417](https://doi.org/10.1103/PhysRevB.88.075417)

PACS number(s): 71.20.Tx

I. INTRODUCTION

Intermolecular electronic wave function overlap and the consequent band formation is the key to enhanced charge transfer/transport properties in molecular materials.^{1,2} Recently, nearly free-electron (NFE) bands were discovered in several two-dimensional molecular overlayers on metal surfaces.^{1,3,4} In-depth investigations have revealed that generally the NFE behavior has the origin in the perturbation of the surface bands of the metal substrate by the molecular overlayer rather than being of purely molecular origin.^{3,4} It is significant, therefore, that molecular NFE properties have been discovered in bands formed by one-dimensional to three-dimensional nanostructures of C₆₀ molecules.⁵ This intrinsic NFE character arises from the superatom molecular orbitals (SAMOs) of hollow molecules.⁵⁻⁷ SAMOs of C₆₀ molecules have been discovered by atomically resolved scanning tunneling microscopy (STM) imaging, and their universal existence in hollow molecules has been established by electronic structure theory.⁸⁻¹⁸ Unlike the typical π -symmetry valence orbitals (mainly composed of the carbon 2*s*, 2*p* atomic orbitals), which are spatially confined to the carbon cage by the carbon atomic potential, the SAMOs originate from the central exchange-correlation potential due to polarization of all the constituent atoms forming the hollow shell. They have atomlike spherical harmonic probability distributions with substantial charge density within the hollow core. Their diffuse density, which extends substantially beyond the molecular van der Waals radius, allows them to readily hybridize among neighboring molecules to form NFE bands similar to those of free-electron metals, e.g., alkali metals. We have recently discovered SAMO-like orbitals even in planar aromatic molecules such as C₆F₆,¹⁹ which also form NFE bands.^{20,21} The universal character of such atomlike states forming NFE bands in quantum structures of hollow spherical and planar molecules invites discovery of optimized materials with possible applications in molecular electronics.

Despite the attractive prospect of utilizing the NFE bands of fullerenes for charge transport in molecular electronics, the high energy of the SAMOs [$>3\text{eV}$ above the lowest-unoccupied molecular orbital (LUMO) in the case of C₆₀] preclude such applications.⁵ Only the frontier orbitals participate in charge-transport applications; therefore, the energy of SAMOs should be reduced so that it is either the highest-occupied molecular orbital (HOMO) or the LUMO. In order to stabilize the SAMOs relative to the LUMOs, we have explored by theory different strategies, such as endohedral and exohedral doping, or tuning the molecular electronic structure through application of an external electric field.⁶ We found the endohedral doping of metal atoms into the fullerene cage to be the most effective approach to SAMO stabilization, because of the effective hybridization between *s*-SAMO and *s*-symmetry valence state of the metal atom.^{5,6} Such interaction creates hybrid states that share the atomlike properties of the parent orbitals, with the bonding component having lower energy than either of the parent orbitals. The bonding orbital is more diffuse than the parent atomic orbital of the endohedral atom (EA), and thus can enhance intermolecular orbital interactions. In this paper, we provide experimental evidence for such hybrid molecular orbitals within the endohedral metallofullerene, La@C₈₂. The La@C₈₂ molecule is chosen because among endohedral metallofullerenes, it is readily available and extensively studied. We show that the inclusion of the La atom within the fullerene cage lowers the *s*-SAMO energy by about 2 eV with respect to that of C₆₀. In addition, we find that upon adsorption on metal surfaces, in our case, Cu(111), the *s*-SAMO level of La@C₈₂ molecules moves further toward Fermi level (E_f), making the *s*-SAMO the first unoccupied state of La@C₈₂ that is detectable by STM (the localized La 4*f* state-derived LUMO is screened by the fullerene cage, which makes it difficult to observe). We present experimental STM measurements and electronic structure calculations that enable identification of SAMOs among complex electronic

resonances of endohedral metallofullerenes and discuss more broadly how the endohedral doping perturbs the SAMOs in different materials beyond La@C₈₂.

The rest of the paper is organized as follows. We describe in Sec. II. A and Sec. II. B the experimental techniques and some details of the density functional theory (DFT) calculations. In Sec. III we provide a general picture of the electronic structure of endohedral metallofullerenes, which will be used to interpret the experimental results in the following sections. Section IV gives the electronic structure of La@C₈₂ molecules determined by STM experiments and DFT calculations. In particular, we show how to assign and differentiate the observed resonances in the measured spectra, including the fullerene cage localized π^* -character states, SAMOs, and states with primarily La character in La@C₈₂ molecules. Section V focuses on the energy stabilization of *s*-SAMO of La@C₈₂ molecules, by comparing resonance positions of fullerenes with those of an empty cage. A general discussion for understanding of the endohedral doping effect on the SAMOs of other endohedral metallofullerenes is then presented. The effects of a metal substrate on the SAMOs are also briefly discussed. Finally, the summary and conclusions are given.

II. EXPERIMENTAL AND THEORETICAL METHODS

A. Experimental methods

We investigate the electronic structure of La@C₈₂ molecules directly adsorbed on Cu(111) surface and on a buffer consisting of a C₆₀ monolayer on Cu(111) surface [C₆₀/Cu(111)]. The two types of surfaces are used to characterize the interaction of La@C₈₂ with the metal substrate. The predeposited C₆₀ monolayer on the Cu(111) surface isolates La@C₈₂ molecules from direct contact with, and therefore, charge transfer from the metal substrate.²² We explore the electronic properties of La@C₈₂ molecules by recording the constant-distance differential conductance spectra (dI/dV) with a lock-in amplifier and the constant-current distance-voltage [$z(V)$] scans. The latter are numerically converted into $d(\ln z)/d(\ln V)$ spectra.^{5,23} The dI/dV method is the standard approach for recording the local electronic structures at the atomic scale by STM. For dI/dV measurements performed at a constant-height, as the voltage is ramped, the tunneling current rises exponentially. Large current, however, can saturate the measurement electronics or destroy the sample, limiting the ability to detect high-energy (e.g., >3 V) resonances.^{24–26} Such limits are overcome in $z(V)$ measurements because the tunneling current is fixed. This allows measurements to be performed at a higher bias voltage than in the constant-height mode.^{27–29} As the tip moves farther from the surface during ramping of the voltage, extracting density-of-states (DOS) information from $z(V)$ spectra is not as well established as for dI/dV spectra.²³ In the region of overlap, $d(\ln z)/d(\ln V)$ spectra, however, have shown to reproduce the peak positions obtained by dI/dV within 0.1 eV, where the differences can be attributed to different strengths of the applied fields.^{23,30} We perform complementary measurements of the electronic structure of La@C₈₂ molecules using both methods.

Within La@C₈₂ molecules, La atoms are displaced from the center of the C₈₂ cage due to charge transfer and the consequent Coulomb attraction of up to three valence electrons from La to the fullerene cage. Therefore, upon adsorption La atoms could be located at different positions with respect to the substrate. We note that we do not find significant variation in spectroscopic measurements performed on different molecules, indicating that either all molecules have the EA in the same location or the molecular conductivity is insensitive to it. Moreover, the tunneling current exhibits no evidence of the internal La atom motion that has been predicted based on x-ray diffraction data and theory.^{31–33} In the case of Sc₃N@C₈₀, we discovered the tunneling electron-induced rotational motion of Sc₃N cluster through characteristic telegraph noise that is imprinted on the tunneling current,^{34,35} but in the case of La@C₈₂, similar current fluctuations that could arise through La motion among several stable sites are not observed. Unlike Li@C₆₀, for which the internal Li atom motion has been predicted,³⁶ single electron scattering through unoccupied resonances of the multiply charged La within the C₈₂ cage is less likely to provoke the EA motion.

The structural and spectroscopic measurements are performed at 77 K in an Omicron LT-STM with a base pressure below 10^{−10} mbar. A Cu(111) crystal is cleaned by cycles of Ar⁺ sputtering followed by annealing to ~ 700 K. C₆₀ molecules are commercially obtained (99% purity; Aldrich), while La@C₈₂ molecules are synthesized and purified as described in Ref. 37. Both molecules are thermally evaporated onto the substrate with a self-made resistively heated evaporator. In order to form compact C₆₀ islands with uniform adsorption structures, the Cu(111) surface is kept at 450 K, while C₆₀ molecules are evaporated,³⁸ followed by postdeposition annealing at 500 K. During the molecular deposition, the Cu(111) and C₆₀/Cu(111) substrates are kept at room temperature.

B. Theoretical methods

DFT calculations of the electronic structure of La@C₈₂ molecule are performed using the Vienna *Ab initio* Simulation Package code with a well-converged 400-eV plane-wave cutoff,³⁹ the Perdew-Wang 1991 functional,⁴⁰ and the projector-augmented wave method. For the calculation of the electronic structure of a free La@C₈₂ molecule, we use a cubic unit cell with dimension $a = 30$ Å. The La@C₈₂ molecule is assembled by placing a La atom into the cage of the C₈₂ isomer with C_{2v} symmetry. In the optimized geometry, the La atom lies along a C₂ axis above a six-membered ring of the C₈₂ cage. The distance between the La atom and the nearest C atoms is 2.52 Å (the average radius of the empty cage is ~ 3.8 Å), in good agreement with the experimental value of 2.55 Å.³¹

III. THE ELECTRONIC STRUCTURE OF ENDOHEDRAL METALLOFULLERENES

Before presenting our results, we discuss general features of the electronic structure of endohedral metallofullerenes. According to the charge density distributions, the unoccupied states of an empty fullerene can be classified as the π^* states localized on the carbon cage (e.g., LUMO + n series, also referred to as the “cage states”) and the diffuse SAMOs. The

local DOS (LDOS) images of π^* states typically display intramolecular contrast on the scale of several angstroms corresponding to the dimensions of pentagons and hexagons of the fullerene cage⁴¹ and reflecting the nodal structure of the π^* orbitals. By contrast, SAMOs have smoother LDOS extending over the entire fullerene cage with the atomlike nodal structure of spherical harmonics characterized by the orbital quantum number l .⁵ Inclusion of an EA introduces a third type of state, which we refer to as the EA states.⁴² The EA states are derived mainly from the atomic orbitals of the EA; they can mix with both cage states and the SAMOs. Although our nomenclature is based on the unperturbed electronic structure of the fullerene cage and the La atom, it should be understood that some degree of mixing exists among these states.⁴³

General features of the endohedral metallofullerene electronic structure can be appreciated from how the EA potential contributes to that of the fullerene cage. We first discuss how the EA perturbs the π^* states. An EA causes some charge transfer depending on its ionization potential and the electron affinity of fullerene.^{44–50} For low ionization potential EA, the charge is transferred from EA to the LUMO of the cage such that the E_f of the combined system is within the LUMO.⁵ Consequently, by comparing the STM spectra of a fullerene with and without the EA, a *rigid* shift of the LUMO states with respect to E_f is expected. The charge transfer and the consequent Coulomb interaction cause EA to adsorb on the inner wall of the cage, when the ionic radius of EA is much smaller than the effective inner radius of the cage. For an EA with high ionization potential, such as rare gas atoms,⁵¹ there is essentially no charge transfer, and the LUMO states remain empty; the neutral EA then resides at the cage center. In both cases, the EA provides an attractive potential, which lowers all energy levels of the fullerene. For π^* states, which are mostly localized on carbon atoms, the energy shifts due to this potential are similar whether the EA is at or displaced from the cage center.

In contrast to the π^* states, the SAMOs are strongly affected by the presence and location of the EA. The diffuse SAMOs experience simultaneously the potentials of the hollow fullerene core as well as the metal atom. The response of SAMOs depends strongly on their symmetry and spatial distribution. The s -SAMO of the interacting system is strongly stabilized with respect to that of the empty cage because its density is mostly confined within the cage, where it strongly overlaps with the unoccupied $6s$ La orbital, which lies at a lower energy. DFT calculations of the C_{60} molecule endohedrally doped with alkali, alkaline earth, noble, and rare-earth metal atoms exhibit a nearly linear relation between energy of the s -SAMO state of the combined system with respect to E_f and the ionization potential of the free metal atoms (representing the binding energy of the frontier s -symmetry state).⁶ Specifically, the energy stabilization of the s -SAMO state depends mainly on strength of the endohedral atomic potential. Figure 1 shows the anticorrelation of the s -SAMO energy with the atomic first ionization potential for EA placed in the center of C_{60} molecule. Further analysis shows that the resulting s -SAMO is mainly derived from the s orbital of the EA: i.e., it is more localized than s -SAMO of the empty cage because of the EA atomic potential, but the SAMO admixture imparts some diffuse character.

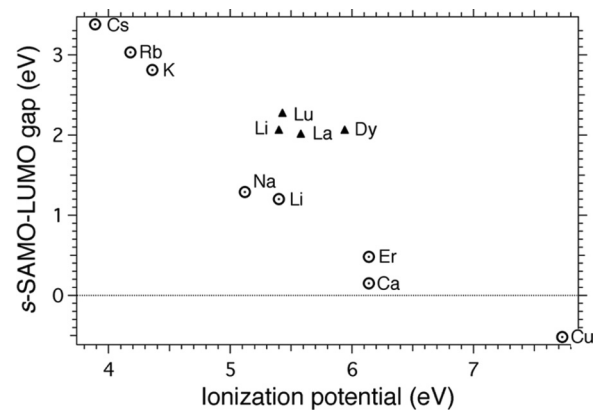


FIG. 1. The anticorrelation between the s -SAMO energies calculated by DFT of $M@C_{60}$ molecules with different metal atoms, M , placed at the center of fullerene vs the first ionization potential of M . The data points for La, Dy, and Lu represent the energies from spectroscopic STM measurements (filled triangles), which we attribute to the s -SAMO.^{42,65} For these measurements, the metal atoms are presumed to be at their equilibrium positions within $M@C_{82}$ molecules. For an estimate of the destabilization of s -SAMO due to the displacement of EA from the cage center, the calculated equilibrium value of s -SAMO for $Li@C_{60}$ is also given (filled triangle).

Compared with the s -SAMOs, the hybrid p -SAMOs are more diffuse, because for the empty cage they reside predominantly outside the cage where they are less affected by EA potential. Moreover, the s and p states of EA are separated by the atomic s - p gap, which is generally larger than the SAMO s - p gap of 0.56 eV.^{5,7} The atomic p state can actually be above the p -SAMO so that the bonding hybrid state formed by their interaction has predominantly a p -SAMO character. Therefore, the stabilization of the p -SAMO is relatively small and its wave function is more diffuse than the s -SAMO. These general features are illustrated by $Li@C_{60}$,⁵ where Li donates one electron to C_{60} , causing a rigid shift of the π^* states. Placing Li at the center of C_{60} metallofullerene stabilizes the hybrid s -SAMO from 3.5 eV for the empty C_{60} above LUMO to 1.2 eV, as shown in Fig. 1. At equilibrium, however, the Li atom is displaced from the center of C_{60} , and consequently the s -SAMO energy is raised by 0.85 eV from its minimum value at the center. The p -SAMO for the off-center Li position is 1.8 eV above the s -SAMO.

IV. EXPERIMENTAL AND THEORETICAL ELECTRONIC STRUCTURE OF $La@C_{82}$

A. STM images and spectra

In this subsection, we present STM results on the adsorption behavior and electronic structure of $La@C_{82}$ on $C_{60}/Cu(111)$ and $Cu(111)$ surfaces. C_{60} molecules form well-ordered, 3×3 close-packed overlayers on $Cu(111)$ terraces.³⁸ Defects in the overlayer form at the boundaries between C_{60} domains with different orientations or belonging to different terraces. Such defects are the preferred sites for $La@C_{82}$ molecule adsorption on C_{60} monolayers. In Fig. 2(a), we observe three $La@C_{82}$ molecules, which appear as bright contrast at the domain boundary defects. We conclude that at 300 K, $La@C_{82}$

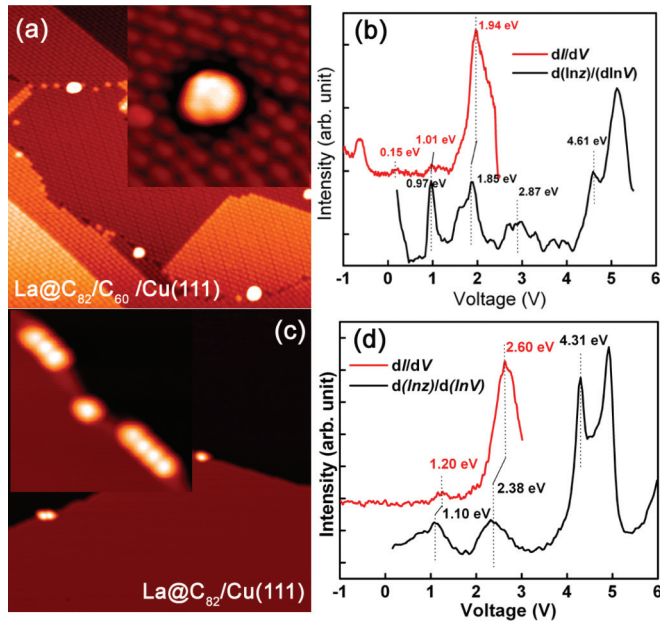


FIG. 2. (Color online) (a) STM topographic images of La@C_{82} molecules on the $\text{C}_{60}/\text{Cu}(111)$ substrate. Isolated La@C_{82} molecules are located at interfaces between differently oriented C_{60} domains or interfaces of domains on different terraces. The image size is 50×50 nm. The inset (3.8×3.8 nm) shows an enlarged image of a single La@C_{82} molecule. (b) Combined dI/dV and $d(\ln z)/d(\ln V)$ spectra obtained for a single isolated La@C_{82} molecule. Below 3 eV, the peaks in dI/dV spectra coincide with those of $d(\ln z)/d(\ln V)$. (c) and (d) STM topographic image (50×50 nm) as well as combined dI/dV and $d(\ln z)/d(\ln V)$ spectra of La@C_{82} molecules adsorbed on the $\text{Cu}(111)$ step edge. Single La@C_{82} molecules and assemblies of several molecules are located at step edges on the lower terrace. The inset (12×12 nm) shows a single La@C_{82} molecule, a trimer, and a quadrimer. The dI/dV and $d(\ln z)/d(\ln V)$ spectra in (b) and (d) are combined using an arbitrary vertical scale.

molecules are mobile on the C_{60} monolayer and easily diffuse to the more stable defect adsorption sites.

Figure 2(b) shows typical dI/dV and $d(\ln z)/d(\ln V)$ spectra of La@C_{82} obtained for the same molecules and STM tip. The dI/dV spectra reveal molecular electronic resonances near E_f , whereas the $d(\ln z)/d(\ln V)$ spectra extend to higher energies. In the region of overlap, both spectra show resonances corresponding to the same electronic states but at slightly different energies and with different relative intensities. For example, two weak resonances, one centered at 0.15 eV and straddling the E_f , and the other at 1.01 eV, and one strong resonance at 1.94 eV appear in dI/dV spectra. The $d(\ln z)/d(\ln V)$ spectra locate two of the three resonances at 0.97 and 1.85 eV. Resonances crossing E_f cannot be detected in $z(V)$ measurements because the constant current condition cannot be obtained at zero bias. For the occupied states, the measured dI/dV spectra on single molecules are consistent with the previous measurements on the La@C_{82} multilayer islands by Taninaka *et al.*⁵² There are, however, some minor differences for the unoccupied states.⁵² A state straddling E_f is resolved in our measurement, which is consistent with the existence of a half-filled singly occupied molecular orbital (SOMO) of La@C_{82} molecules.^{47,48} In La@C_{82} multilayers,

such states split because crystal field interactions in the solid state introduce a band gap.^{47,52}

Figure 2(c) shows a typical STM topographic image of the $\text{La@C}_{82}/\text{Cu}(111)$ surface. At low coverages, La@C_{82} molecules adsorb at steps on the lower terrace as isolated as monomers, dimers, trimers, and longer aggregates aligned along the step edges. This is consistent with previous reports of STM imaging of endohedral fullerenes.^{53–55} Figure 2(d) presents the combined dI/dV and $d(\ln z)/d(\ln V)$ spectra acquired above La@C_{82} monomers adsorbed on the $\text{Cu}(111)$ surface.

Comparing the spectra of the two samples, we notice that the three resonances in Fig. 2(d) can be associated with the similar progression in Fig. 2(b), by assuming a nearly rigid energy downshift toward E_f for molecules in direct contact with the metal substrate. Specifically, we associate the resonances of La@C_{82} at 1.1, 2.38, and 4.31 eV on the $\text{Cu}(111)$ substrate with the resonances found at 1.85, 2.87, and 4.61 eV on the C_{60} buffer layer. The energy downshift due to interaction with the substrate for the lower-energy resonances is ~ 0.6 – 0.7 eV. The rigid shift implies that these states are affected by the same mechanism. The energy shift of the 4.5 eV resonance is less than the lower-energy resonances; however, the origin of the difference is not clear. In addition, the adsorption directly on the $\text{Cu}(111)$ surface causes the two resonances (0.15 and 1.01 eV) near E_f for La@C_{82} on the C_{60} buffer layer to disappear. This behavior is consistent with the π^* origin of these two states. The π^* states of the cage can couple strongly with the metal substrate, causing them to broaden into resonances, which are difficult to detect. The SAMOs or La-derived states, by contrast, interact more weakly with the metal substrate, and therefore experience less broadening, because their defining potentials are shielded within the hollow fullerene core. In the following, we present more evidence to support these conclusions.

B. Identification of the SAMO and EA states

In this subsection, we identify the observed resonances of La@C_{82} molecules by combining the experimental results with the DFT calculations. We find good agreement between experimental and theoretical results, in particular, the assignment of s -SAMO. The calculated DOS of La@C_{82} displays many peaks (Fig. 3), among which we focus on the SAMOs and La-derived states. Our DFT calculations reveal four empty noncage states. They are in the increasing energy order La $4f$, with the electronic configuration of La as $[\text{Xe}] 5d^1 6s^2$, s -SAMO (mainly composed of La $6s$ component), La $5d$, and p -SAMO (see Fig. 3). The fact that La $6s$ and $5d$ orbitals are empty is consistent with donation of three electrons from La to C_{82} cage.^{44–49} The SAMOs are identified by analyzing the distribution and symmetry (nodes) of their wave functions.^{5,6}

In Fig. 3, we place the experimental STS spectra, marked with the two already identified π^* cage states, below the calculated DOS. The p -SAMOs can be robustly identified experimentally from their STM LDOS images (see Supplemental Material,⁵⁶ Fig. S1), which reflect the symmetry and diffuse nature of their wave functions. We notice that p -SAMO can also be robustly assigned in $\text{Sc}_3\text{N@C}_{80}$ molecules by using STM LDOS imaging method.¹⁷ The characteristic

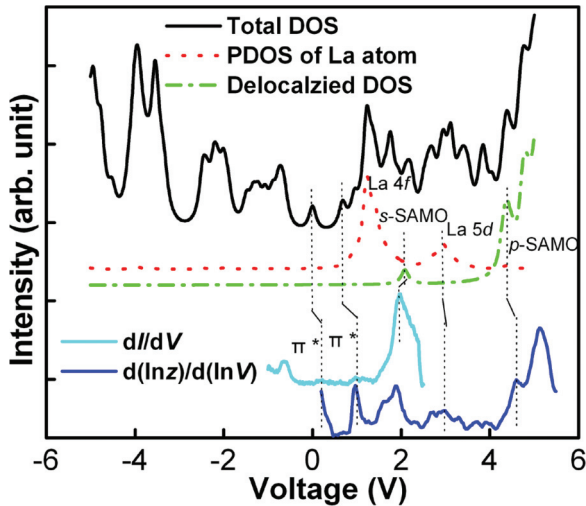


FIG. 3. (Color online) Comparisons between the calculated total DOS of La@C_{82} molecule (black), the projected DOS on La $4f$ and $5d$ (red dotted) and the projected DOS of SAMOs (green dash-dotted) with the experimental dI/dV and $d(\ln z)/d(\ln V)$ spectra (light and dark blue) obtained on isolated La@C_{82} molecules adsorbed on $\text{C}_{60}/\text{Cu}(111)$. The calculated s -SAMO is ~ 2.09 eV above the E_f . There is good agreement in peak positions between the experimental and theoretical data.

appearance of p -SAMOs can be attributed to the fact that most of their density resides outside of the cage, where it is not strongly affected by the endohedral inclusion. By comparing the experimental and theoretical results, with the above information, we can immediately assign the 1.8-eV resonance as s -SAMO and 2.9-eV resonance as the La $5d$ state; the agreement with the theoretically predicted energies is within 0.3 eV for the observed resonances. The observed energy is also consistent with the relationship between the atomic ionization potential and the s -SAMO energy in Fig. 1, if one accounts for the destabilization of s -SAMO by the displacement of the La atom from the center of the cage. The only discrepancy between the experimental spectra and the electronic structure calculations is the La $4f$ resonance, which is calculated at 1.25 eV, but does not appear in the STS measurements. We argue that the La $4f$ resonance is difficult to detect by tunneling spectroscopy because its wave function is compact and mostly confined inside the cage, as predicted by theory. Otherwise, there is good agreement in Fig. 3 between the experimentally observed and theoretically predicted resonance energies.

The assignments of the s -SAMO (having a large La $6s$ component) and La $5d$ state are also consistent with other experimental findings. First, LDOS images at 1.8- and 2.9-eV resonances lack sharp intramolecular contrast (Supplemental Material,⁵⁶ Fig. S2), from which we rule out that they are the localized cage states. Furthermore, by comparing the position-dependent dI/dV spectra (Supplemental Material,⁵⁶ Fig. S3), we find that the intensity of the low-energy resonance (1.8 eV) is insensitive to the measurement location, whereas that of the higher-energy resonance (2.9 eV) is more strongly position dependent. These results indicate the lower-energy resonance has a more uniform azimuthal dependence than the higher energy one and confirms its s -SAMO character. The

higher-energy resonance, assigned as the La $5d$ state, has a stronger azimuthal dependence. Although this state also has some d -SAMO character, apparently the admixture is insufficient to give it a strongly diffuse appearance.

V. ENERGY STABILIZATION OF SAMO

A. The effect of endohedral La

In this subsection, we combine the existing experimental data for isolated C_{60} and La@C_{82} with the DFT calculations to show that the endohedral La indeed lowers the energy of s -SAMO resonance by as much as 2 eV with respect to the empty fullerene cage. Because there is no experimental data on the electronic structure of the empty C_{82} cage, we are not able to make a direct assessment of the effect of the EA. Instead, we offer two indirect comparisons that reach the same conclusion. First, we compare the DFT results for La@C_{82} and empty C_{82} , assuming that the good agreement with experiment for La@C_{82} will also hold for the empty C_{82} . Second, by assuming SAMOs of the empty C_{60} and C_{82} are similar, we compare the

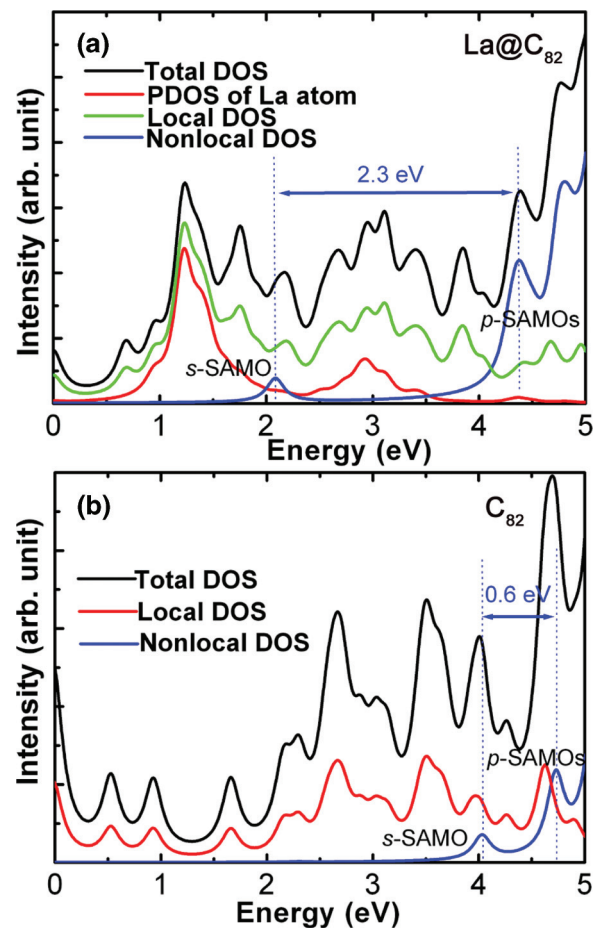


FIG. 4. (Color online) The calculated total, local, and nonlocal DOS of isolated La@C_{82} (a) and C_{82} (b). The s - and p -SAMOs belong to the nonlocal DOS. The strong influence of La^{3+} on the s -SAMO results in an s - p SAMO splitting of ~ 2.3 eV in the case of La@C_{82} , whereas it is only ~ 0.6 eV for the empty C_{82} . Compared with s -SAMO, the p -SAMOs are less affected by the presence of La^{3+} inside the cage.

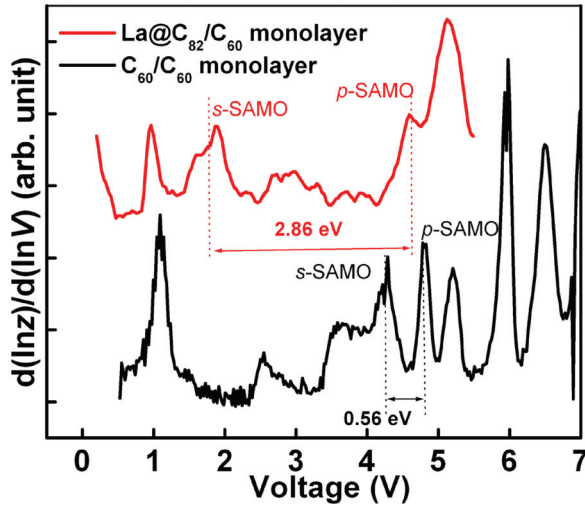


FIG. 5. (Color online) The energy difference between the *s*- and *p*-SAMOs of isolated La@C_{82} and C_{60} molecules on a C_{60} buffer layer. For the La@C_{82} molecule, the energy difference is 2.86 eV, whereas for the isolated C_{60} , it is 0.56 eV.

electronic structure revealed by the STM spectra of the empty C_{60} and La@C_{82} .

The calculated local, nonlocal, and total DOS of isolated La@C_{82} and isolated C_{82} molecules are presented in Figs. 4(a) and 4(b). It is evident that La^{3+} inside the carbon cage greatly stabilizes the *s*-SAMO but has a much smaller effect on the *p*-SAMOs. Not having a C_{82} sample, we analyze the stabilization effect of La on the SAMOs by using C_{60} molecule as a reference. The C_{60} and C_{82} cages support SAMOs with quite similar properties, except that the binding energy of the *s*-SAMO for C_{82} with respect to vacuum energy is predicted by DFT calculations to be ~ 0.27 eV larger than for C_{60} on account of its larger cage.⁶ Comparing the SAMOs of a La@C_{82} molecule on the C_{60} monolayer with a C_{60} molecule on the C_{60} monolayer (Fig. 5), we find that (i) the *s*-SAMO in La@C_{82} is much closer to the E_f and (ii) the energy difference between *s*- and *p*-SAMOs in La@C_{82} (2.86 eV) is much larger than that for C_{60} molecules (0.56 eV). These *s*-*p* gaps are quite comparable to the calculated ones for La@C_{82} and C_{82} , indicating that the experimental comparison between La@C_{82} and C_{60} is reasonable. This analysis leads us to conclude that the *s*-SAMO is stabilized by nearly 2 eV by hybridization with the $6s$ state of endohedral La^{3+} ion. At the same time, we find that the apparently weaker interaction between *p*-SAMOs with the higher-energy $6p$ state of La^{3+} stabilizes *p*-SAMO by only around 0.5 eV.

Our results confirm that the stabilization of the *s*-SAMO is realized by introducing La into the carbon cage, whereas the *p*-SAMO is less affected. Such stabilization has been predicted by DFT calculations, and a simple picture is given in Sec. III. Our measurements and spectroscopic assignments give clear evidence for *s*-SAMO stabilization by EAs. Similar conclusions can be drawn by extending our analysis of the electronic spectra of other endohedral fullerenes, which have been previously reported in the literature, as will be elaborated at the end of this section.

B. The effect of metal substrates

Finally, we discuss the influence of metal substrate on the SAMO energies. Our results indicate that interaction between the La@C_{82} molecules and the metal substrate provides another mechanism for stabilizing the SAMOs. Interpreting the La@C_{82} -Cu(111) substrate interaction is complicated by the uncertain structure of the interface.^{32,57,58} It has been reported that adsorption of endohedral metallofullerene molecules can cause a reconstruction of the metal atoms underneath the molecules on Cu(111) surface.⁵⁹ Depending on the deposition and annealing conditions, C_{60} molecules can displace metal atoms to dimple the surface.⁶⁰ In the particular case of our measurements, the molecules are adsorbed on step edges where the local surface structure might have a particular effect on the molecule-substrate interaction.

Despite the uncertainty of the molecule/metal interface structure, we observe similar substrate effect on SAMOs of C_{60} as for La@C_{82} molecules. Figures 6(a) and 6(b) show the STS of La@C_{82} and C_{60} molecules on the C_{60} monolayer/Cu(111) and Cu(111) surfaces. Comparing the spectra in Figs. 6(a) and

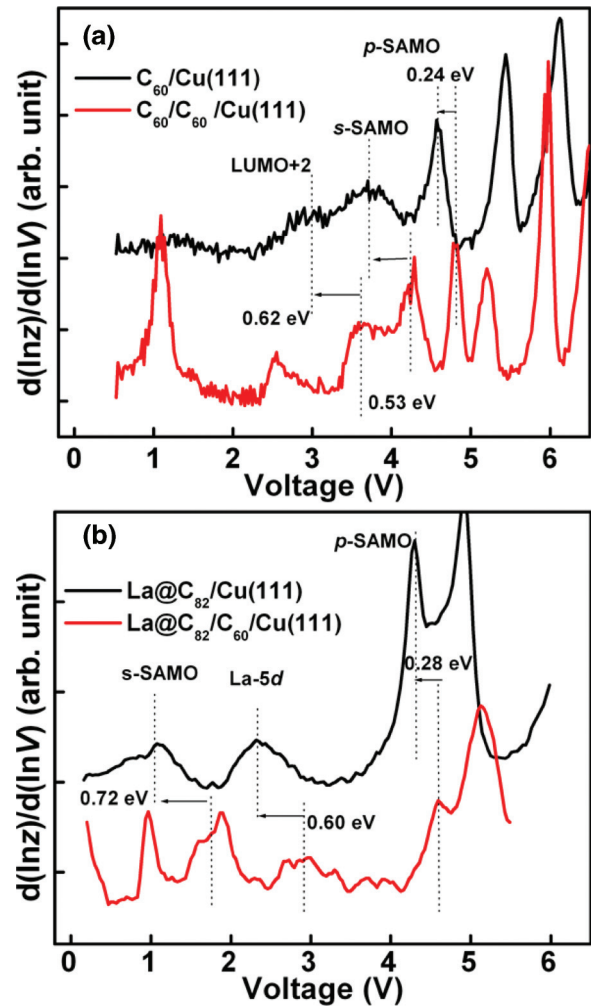


FIG. 6. (Color online) The Cu(111) substrate effect on the SAMOs. (a) $d(\ln z)/d(\ln V)$ spectra of C_{60} on Cu(111) and $\text{C}_{60}/\text{Cu}(111)$ surfaces. (b) $d(\ln z)/d(\ln V)$ spectra of La@C_{82} on Cu(111) and $\text{C}_{60}/\text{Cu}(111)$ surfaces. In both cases, the energy levels shift down in the presence of the Cu(111) substrate.

6(b), we see similar energy downshift for the *s*-SAMO and other resonances (LUMO + 2 or La 5*d*) at proximate energies to the *s*-SAMO when both fullerenes are adsorbed on Cu(111). This suggests that similar mechanism is involved in the stabilization by the metal substrate. The interaction between C₆₀ molecules and Cu(111) has been extensively studied and interpreted.^{61,62} Charge transfer from the Cu(111) substrate to C₆₀ is the primary manifestation of their interaction. A charge transfer of 0.8 electrons^{61,63} can be attributed to the image-charge interaction,⁶⁴ which causes a rigid downshift of C₆₀ electronic states; when the LUMO of free C₆₀ molecule is depressed below E_f , the charge flows from the metal surface to C₆₀ molecule. In the case of La@C₈₂, although the C₈₂ cage receives three electrons from La atom even before chemisorption,^{44–49} further charge transfer is possible to the partially occupied SOMO state.

Through the interaction with the metal substrate, the *s*-SAMO becomes the lowest-unoccupied state that can be detected in the STM spectroscopic measurements. The La 4*f* state is predicted to be below *s*-SAMO, but its localized nature within the cage hinders observation in a STM measurement. This result suggests that an EA with similar ionization potential to La, but without low energy, unoccupied 4*f* states might stabilize the *s*-SAMO to make it the LUMO of endohedral metallofullerene at interface with a metal.

C. Comparison with other endohedral fullerenes

The unoccupied electronic structures of Dy@C₈₂ and Lu@C₈₂ molecules based on dI/dV spectroscopy also have been reported in the literature.^{42,65} In these studies only LUMO or EA states were considered as possible candidates for the spectroscopic assignments, because the SAMOs had not yet been discovered. The Dy 6*s* state was reported to be at ~ 2.04 eV above E_f .⁴² Based on the anticorrelation in Fig. 1, however, we can assign it to the *s*-SAMO of Dy@C₈₂ according to the ionization potential of Dy and the expectation that the 6*s* state will hybridize with the *s*-SAMO. We can make a similar assignment to the 2.3-eV resonance found in the case of Lu@C₈₂.⁶⁵ We note that in Lu@C₈₂ molecules, Lu atoms with the electronic configuration [Xe] 6*s*²4*f*¹⁴5*d*¹ donate approximately three electrons to the cage.⁶⁶ In this case, the Lu³⁺ ion has a closed shell with the 4*f* states being fully occupied. Therefore, the LUMO is a cage state and the LUMO + 1 is the stabilized *s*-SAMO.⁶⁵ If the charge transfer from the substrate to Lu@C₈₂ is sufficient to fully occupy the LUMO of the free molecule, then the *s*-SAMO

becomes the LUMO of the chemisorbed Lu@C₈₂ /substrate system. This will, in general, be the case for EAs with closed shell configurations, which donate their valence electrons to the fullerene cage. In the case that endohedral fullerenes contain clusters rather than atomic inclusions, we expect similar interactions to occur between the unoccupied orbitals of the cluster and SAMOs of the fullerene cage, with potentially novel outcomes. Indeed, we found such hybrid SAMOs in the case of monomers and clusters of Sc₃N@C₈₀ molecules.^{17,67,68}

VI. CONCLUSIONS

In conclusion, by combining STM spectroscopic measurements with DFT electronic structure calculations, we have demonstrated that *s*-SAMO of C₈₂ fullerene is lowered by about 2 eV through the interaction with the endohedral La atom. The influence of the metal substrate further stabilizes the *s*-SAMO energy to ~ 1 eV above the Fermi level. The first phenomenon can be understood as a consequence of orbital hybridization between the C₈₂ SAMOs and the internal atoms. The degree of stabilization is directly related to the ionization potential of the endohedral metal atom.⁶ The second phenomenon is a substrate screening effect, which further modifies the properties of the fullerene-metal interface. Therefore, our result show that the judicious doping of fullerenes with atoms that have the appropriate electronic structure can stabilize the *s*-SAMO so that it is a frontier orbital, and its bands can contribute to NFE transport of nanostructures and solids formed of such molecular solids. Our experimental findings confirm that endohedral metallofullerene molecules doped with high ionization potential metal atoms, such as Er and Cu, have the potential of stabilizing the *s*-SAMO state with NFE properties to near E_f .⁶

ACKNOWLEDGMENTS

The research on superatom states was funded by Division of Chemical Sciences, Geosciences, and Biosciences, Office of Basic Energy Sciences of the U.S. Department of Energy (DOE) through Grant No. DE-FG02-09ER16056 and the STM instrumentation by the Keck Foundation grant. The calculations were performed in the Environmental Molecular Sciences Laboratory at the Pacific Northwest National Laboratory, a user facility sponsored by the DOE Office of Biological and Environmental Research. S.Y. was supported by the National Natural Science Foundation of China (Grant No. 90921013).

*Present address: Department of Physics, University of Texas at Austin, Austin, Texas 78712, USA.

†Corresponding author: petek@pitt.edu

¹R. Temirov, S. Soubatch, A. Luican, and F. S. Tautz, *Nature (London)* **444**, 350 (2006).

²F. S. Tautz, *Prog. Surf. Sci.* **82**, 479 (2007).

³J. Zirosso, F. Forster, A. Schöll, P. Puschnig, and F. Reinert, *Phys. Rev. Lett.* **104**, 233004 (2010).

⁴N. Gonzalez-Lakunza, I. Fernández-Torrente, K. J. Franke, N. Lorente, A. Arnau, and J. I. Pascual, *Phys. Rev. Lett.* **100**, 156805 (2008).

⁵M. Feng, J. Zhao, and H. Petek, *Science* **320**, 359 (2008).

⁶J. Zhao, M. Feng, J. L. Yang, and H. Petek, *ACS Nano* **3**, 853 (2009).

⁷M. Feng, J. Zhao, T. Huang, X. Zhu, and H. Petek, *Acc. Chem. Res.* **44**, 360 (2011).

- ⁸X. Blase, A. Rubio, S. G. Louie, and M. L. Cohen, *Phys. Rev. B* **51**, 6868 (1995).
- ⁹M. Posternak, A. Baldereschi, A. J. Freeman, E. Wimmer, and M. Weinert, *Phys. Rev. Lett.* **50**, 761 (1983).
- ¹⁰X. Blase, A. Rubio, S. G. Louie, and M. L. Cohen, *Europhys. Lett.* **28**, 335 (1994).
- ¹¹X. Blase, L. X. Benedict, E. L. Shirley, and S. G. Louie, *Phys. Rev. Lett.* **72**, 1878 (1994).
- ¹²T. Miyake and S. Saito, *Phys. Rev. B* **65**, 165419 (2002).
- ¹³Y. Miyamoto, S. Saito, and D. Tománek, *Phys. Rev. B* **65**, 041402 (2001).
- ¹⁴Y. Miyamoto, A. Rubio, X. Blase, M. L. Cohen, and S. G. Louie, *Phys. Rev. Lett.* **74**, 2993 (1995).
- ¹⁵S. Okada, A. Oshiyama, and S. Saito, *Phys. Rev. B* **62**, 7634 (2000).
- ¹⁶A. Rubio, Y. Miyamoto, X. Blase, M. L. Cohen, and S. G. Louie, *Phys. Rev. B* **53**, 4023 (1996).
- ¹⁷T. Huang, J. Zhao, M. Feng, H. Petek, S. F. Yang, and L. Dunsch, *Phys. Rev. B* **81**, 085434 (2010).
- ¹⁸V. K. Vora, L. S. Cederbaum, and K. D. Jordan, *J. Phys. Chem. Lett.* **4**, 849 (2013).
- ¹⁹D. B. Dougherty, M. Feng, H. Petek, J. T. Yates, and J. Zhao, *Phys. Rev. Lett.* **109**, 266802 (2012).
- ²⁰G. Dutton and X. Y. Zhu, *J. Phys. Chem. B* **105**, 10912 (2001).
- ²¹C. Gahl, K. Ishioka, Q. Zhong, A. Hotzel, and M. Wolf, *Faraday Discuss.* **117**, 191 (2000).
- ²²X. Y. Zhu, G. Dutton, D. P. Quinn, C. D. Lindstrom, N. E. Schultz, and D. G. Truhlar, *Phys. Rev. B* **74**, 241401 (2006).
- ²³A. Pronschinske, D. J. Mardit, and D. B. Dougherty, *Phys. Rev. B* **84**, 205427 (2011).
- ²⁴S. W. Hla and K. H. Rieder, *Annu. Rev. Phys. Chem.* **54**, 307 (2003).
- ²⁵W. Ho, *J. Chem. Phys.* **117**, 11033 (2002).
- ²⁶S. Alavi, R. Rousseau, G. P. Lopinski, R. A. Wolkow, and T. Seideman, *Faraday Discuss.* **117**, 213 (2000).
- ²⁷R. S. Becker, J. A. Golovchenko, and B. S. Swartzentruber, *Phys. Rev. Lett.* **55**, 987 (1985).
- ²⁸G. Binnig, K. H. Frank, H. Fuchs, N. Garcia, B. Reihl, H. Rohrer, F. Salvan, and A. R. Williams, *Phys. Rev. Lett.* **55**, 991 (1985).
- ²⁹D. B. Dougherty, P. Maksymovych, J. Lee, and J. T. Yates, Jr., *Phys. Rev. Lett.* **97**, 236806 (2006).
- ³⁰M. Ziegler, N. Néel, A. Sperl, J. Kröger, and R. Berndt, *Phys. Rev. B* **80**, 125402 (2009).
- ³¹E. Nishibori, M. Takata, M. Sakata, H. Tanaka, M. Hasegawa, and H. Shinohara, *Chem. Phys. Lett.* **330**, 497 (2000).
- ³²W. Andreoni and A. Curioni, *Phys. Rev. Lett.* **77**, 834 (1996).
- ³³S. Sato, H. Nikawa, S. Seki, L. Wang, G. Luo, M. Harannaka, T. Tsuchiya, S. Nagase, and T. Akasaka, *Angew. Chem. Int. Ed.* **51**, 1589 (2012).
- ³⁴T. Huang, J. Zhao, M. Peng, A. A. Popov, S. F. Yang, L. Dunsch, and H. Petek, *Nano Lett.* **11**, 5327 (2011).
- ³⁵T. Huang, J. Zhao, M. Feng, A. A. Popov, S. F. Yang, L. Dunsch, and H. Petek, *Chem. Phys. Lett.* **552**, 1 (2012).
- ³⁶R. Jorn, J. Zhao, H. Petek, and T. Seideman, *ACS Nano* **5**, 7858 (2011).
- ³⁷Y. F. Lian, S. F. Yang, and S. H. Yang, *J. Phys. Chem. B* **106**, 3112 (2002).
- ³⁸T. Hashizume, K. Motai, X. D. Wang, H. Shinohara, Y. Saito, Y. Maruyama, K. Ohno, Y. Kawazoe, Y. Nishina, H. W. Pickering, Y. Kuk, and T. Sakurai, *Phys. Rev. Lett.* **71**, 2959 (1993).
- ³⁹G. Kresse and J. Furthmüller, *Phys. Rev. B* **54**, 11169 (1996).
- ⁴⁰J. P. Perdew, J. A. Chevary, S. H. Vosko, K. A. Jackson, M. R. Pederson, D. J. Singh, and C. Fiolhais, *Phys. Rev. B* **46**, 6671 (1992).
- ⁴¹X. H. Lu, M. Grobis, K. H. Khoo, S. G. Louie, and M. F. Crommie, *Phys. Rev. Lett.* **90**, 096802 (2003).
- ⁴²K. Wang, J. Zhao, S. Yang, L. Chen, Q. Li, B. Wang, S. Yang, J. Yang, J. G. Hou, and Q. Zhu, *Phys. Rev. Lett.* **91**, 185504 (2003).
- ⁴³Note that the *s*-SAMO is not orthogonal to EA states with *s*-symmetry (such as Li 3*s*, La 6*s*, Cu 4*s*), and their overlap (inner product) is typically large. In such cases, we attribute the resulting diffuse states of *s*-symmetry as *s*-SAMOs, although they may have more EA *s*-state character. The *p*-SAMO, however, does not overlap strongly with EA states because its wave function extends beyond the carbon cage. Therefore, the assignment of *p*-SAMO based on its diffuse character is straightforward.
- ⁴⁴H. Shinohara, *Rep. Prog. Phys.* **63**, 843 (2000).
- ⁴⁵S. Nagase, K. Kobayashi, T. Kato, and Y. Achiba, *Chem. Phys. Lett.* **201**, 475 (1993).
- ⁴⁶K. Laasonen, W. Andreoni, and M. Parrinello, *Science* **258**, 1916 (1992).
- ⁴⁷D. M. Poirier, M. Knupfer, J. H. Weaver, W. Andreoni, K. Laasonen, M. Parrinello, D. S. Bethune, K. Kikuchi, and Y. Achiba, *Phys. Rev. B* **49**, 17403 (1994).
- ⁴⁸S. Hino, H. Takahashi, K. Iwasaki, K. Matsumoto, T. Miyazaki, S. Hasegawa, K. Kikuchi, and Y. Achiba, *Phys. Rev. Lett.* **71**, 4261 (1993).
- ⁴⁹B. Kessler, A. Bringer, S. Cramm, C. Schlebusch, W. Eberhardt, S. Suzuki, Y. Achiba, F. Esch, M. Barnaba, and D. Cocco, *Phys. Rev. Lett.* **79**, 2289 (1997).
- ⁵⁰P. J. Bennig, J. L. Martins, J. H. Weaver, L. P. F. Chibante, and R. E. Smalley, *Science* **252**, 1417 (1991).
- ⁵¹M. S. Syamala, R. J. Cross, and M. Saunders, *J. Am. Chem. Soc.* **124**, 6216 (2002).
- ⁵²A. Tanimaka, K. Shino, T. Sugai, S. Heike, Y. Terada, T. Hashizume, and H. Shinohara, *Nano Lett.* **3**, 337 (2003).
- ⁵³S. X. Zhao, J. Zhang, J. Q. Dong, B. K. Yuan, X. H. Qiu, S. Y. Yang, J. Hao, H. Zhang, H. Yuan, G. M. Xing, Y. L. Zhao, and B. Y. Sun, *J. Phys. Chem. C* **115**, 6265 (2011).
- ⁵⁴Y. Hasegawa, Y. Ling, S. Yamazaki, T. Hashizume, H. Shinohara, A. Sakai, H. W. Pickering, and T. Sakurai, *Phys. Rev. B* **56**, 6470 (1997).
- ⁵⁵M. J. Butcher, J. W. Nolan, M. R. C. Hunt, P. H. Beton, L. Dunsch, P. Kuran, P. Geiorgi, and T. J. S. Dennis, *Phys. Rev. B* **64**, 195401 (2001).
- ⁵⁶See Supplemental Material at <http://link.aps.org/supplemental/10.1103/PhysRevB.88.075417> for identifying *p*-SAMOs, *s*-SAMO, and La 5*d* states in La@C82 molecules.
- ⁵⁷S. Nagase, K. Kobayashi, and T. Akasaka, *Bull. Chem. Soc. Jpn.* **69**, 2131 (1996).
- ⁵⁸J. Lu, X. W. Zhang, X. G. Zhao, S. Nagase, and K. Kobayashi, *Chem. Phys. Lett.* **332**, 219 (2000).
- ⁵⁹J. Zhang, S. X. Zhao, B. K. Yuan, K. Deng, B. Y. Sun, and X. H. Qiu, *Surf. Sci.* **606**, 78 (2012).
- ⁶⁰W. W. Pai, C.-L. Hsu, M. C. Lin, K. C. Lin, and T. B. Tang, *Phys. Rev. B* **69**, 125405 (2004).
- ⁶¹X. H. Lu, M. Grobis, K. H. Khoo, S. G. Louie, and M. F. Crommie, *Phys. Rev. B* **70**, 115418 (2004).

- ⁶²M. Grobis, X. Lu, and M. F. Crommie, *Phys. Rev. B* **66**, 161408 (2002).
- ⁶³L. L. Wang and H. P. Cheng, *Phys. Rev. B* **69**, 045404 (2004).
- ⁶⁴J. Zhao, N. Pontius, A. Winkelmann, V. Sametoglu, A. Kubo, A. G. Borisov, D. Sánchez-Portal, V. M. Silkin, E. V. Chulkov, P. M. Echenique, and H. Petek, *Phys. Rev. B* **78**, 085419 (2008).
- ⁶⁵M. Iwamoto, D. Ogawa, Y. Yasutake, Y. Azuma, H. Umemoto, K. Ohashi, N. Izumi, H. Shinohara, and Y. Majima, *J. Phys. Chem. C* **114**, 14704 (2010).
- ⁶⁶H. J. Huang and S. H. Yang, *J. Phys. Chem. Solids* **61**, 1105 (2000).
- ⁶⁷A. A. Popov, L. Zhang, and L. Dunsch, *ACS Nano* **4**, 795 (2010).
- ⁶⁸A. A. Popov, S. F. Yang, and L. Dunsch, *Chem. Rev.* (2013), doi:10.1021/cr300297r.